

24 **Abstract**

25 Spent brewery grains, a by-product of the brewing process, were used as
26 precursor of *biochars* and activated carbons to be applied to the removal of
27 pharmaceuticals from water. *Biochars* were obtained by pyrolysis of the raw materials,
28 while activated carbons were produced by adding a previous chemical activation step.
29 The influence of using different precursors (from distinct fermentation processes),
30 activating agents (potassium hydroxide, sodium hydroxide and phosphoric acid),
31 pyrolysis temperatures, and residence times was assessed. The adsorbents were
32 physicochemically characterized and applied to the removal of the antiepileptic
33 carbamazepine from water. Potassium hydroxide activation produced the materials with
34 the most promising properties and adsorptive removals, with specific surface areas up to
35 $1120 \text{ m}^2 \text{ g}^{-1}$ and maximum adsorption capacities up to $190 \pm 27 \text{ mg g}^{-1}$ in ultrapure
36 water. The adsorption capacity suffered a reduction of $<70\%$ in wastewater, allowing to
37 evaluate the impact of realistic matrices on the efficiency of the materials.

38

39 **Keywords**

40 Brewery wastes; Pyrolysis; Chemical activation; Activated carbon; Pharmaceuticals;
41 Wastewater treatment.

42

43

44

45

46

47

48 **1. Introduction**

49 The use of agricultural and industrial wastes to produce added-value materials is
50 an interesting possibility to reduce the negative impacts of agro-industrial processes,
51 and to reintroduce end-of-life residues into the productive chain (Borel et al., 2018;
52 Jaria et al., 2019). These wastes, usually available in large amounts, can be an
53 alternative to non-renewable sources for being utilized as precursors of carbon
54 materials, such as activated carbons (ACs), to be applied in water purification systems
55 (Azargohar and Dalai, 2008). AC is a carbonaceous material with high adsorption
56 capacity towards a vast number of compounds, such as pharmaceuticals (Jaria et al.,
57 2019). The key properties associated to an AC with high adsorption capacities include
58 high specific surface area (S_{BET}) and microporosity, as well as high carbon and low ash
59 contents (Jaria et al., 2015). For these reasons, agro-industrial lignocellulosic residues,
60 which have low inorganic and relatively high volatile contents, are considered good
61 precursors of AC (Azargohar and Dalai, 2008).

62 Spent brewery grains (SBG) are lignocellulosic wastes which constitute a major
63 by-product of the brewing process, representing around 85% of the total wastes
64 generated by the brewing industry (Borel et al., 2018; Vanreppelen et al., 2014). This
65 material consists of the remains from the barley malt after the mashing process (Barrozo
66 et al., 2019), and their properties depend on the type of used barley and the brewing
67 technology (Olszewski et al., 2019). Nevertheless, their main polysaccharides are
68 generally hemicellulose (mainly arabinoxylane), and cellulose, while lignin and a
69 considerable amount of proteins and lipids are also part of the typical reported
70 composition of SBG (Olszewski et al., 2019; Wierzba et al., 2019). To date, SBG has
71 primarily been used as animal feed (Gonçalves et al., 2017; Vanreppelen et al., 2014).

72 However, considering that the efficient reuse of this agro-industrial waste can be
73 important, not only from the perspective of the brewer who can benefit from the
74 valorization of this by-product, but also from an environmental point of view, the study
75 of alternative SBG applications is highly desirable (Barrozo et al., 2019). In this
76 context, comes up the possibility of using SBG to produce adsorbent materials aiming at
77 the adsorptive removal of water micro-contaminants, such as pharmaceuticals.

78 In the last years, a few studies have reported the possibility to use raw and
79 processed SBG as adsorbent to remove contaminants from water. To the best of the
80 authors' knowledge, the application of SBG to the removal of pharmaceuticals from
81 water has not been so far reported in literature. However, some examples of the
82 application of this material to the removal of other organic pollutants, such as dyes used
83 in paper and textile industries (Fontana et al., 2016; Silva et al., 2004), or inorganic
84 pollutants, such as metals (Ferraz et al., 2005; Wierzba and Andrzej, 2019), from water
85 can be found in literature. Concerning organic contaminants, Silva et al. (2004) studied
86 the removal of acid orange 7, a dye currently used in paper and textile industries, by
87 SBG in aqueous solutions (Silva et al., 2004). The results showed high levels of color
88 removal (above 90%, for an initial dye concentration of 60 mg L⁻¹), with low contact
89 times between adsorbent and dye (less than 1 h), attaining a maximum adsorption
90 capacity of ~30.5 mg g⁻¹, at 30 °C. The reported removal capacity was obtained using
91 the SBG in its raw form, i.e., without any previous treatments such as milling and/or
92 sieving, incineration or chemical modification. Gonçalves et al. (2017) used SBG to
93 produce bio-oil and a granular AC via pyrolysis and CO₂ activation (Gonçalves et al.,
94 2017). In the production of the AC by these authors, the effect of the activation time on
95 some properties, including S_{BET} , was investigated. The adsorptive properties of AC were

96 evaluated by the determination of the iodine number and methylene blue discoloration.
97 The authors concluded that the S_{BET} , iodine number and methylene blue adsorption onto
98 the AC increased as activation time increased. Therefore, six hours of activation
99 resulted in an AC with S_{BET} of $617.4 \text{ m}^2 \text{ g}^{-1}$, an iodine number of 490.1 mg g^{-1} and an
100 excellent adsorption of methylene blue (99.97 % for an initial concentration of 200 mg
101 L^{-1} of methylene blue and granular AC dosage of $10\,000 \text{ mg L}^{-1}$). Ferraz et al. (2005) in
102 a study for Cr (III) adsorption also used SBG as adsorbent, obtaining a maximum
103 adsorption capacity of 17.84 mg g^{-1} at pH 5.0 (Ferraz et al., 2005). As in the study
104 carried out by Silva et al. (2004), this work also reported a good removal capacity of Cr
105 (III) using the SBG in its raw form.

106 Considering the above-mentioned studies and the high availability of SBG for its
107 large-scale application, the use of this biomass as sorbent for the removal of
108 pharmaceuticals from contaminated water could be a sustainable solution for the
109 valorization of this residue, upcycling it through its transformation into an added-value
110 product. The main objective of this work consists of using SBG as a precursor of
111 *biochar* and AC. SBG obtained from two different types of brewing processes was
112 selected to evaluate the impact of the fermentation on the properties of the resulting
113 adsorbents. The produced materials were physical and chemically characterized and
114 subsequently tested as adsorbents to remove the antiepileptic pharmaceutical
115 carbamazepine (CBZ) from aqueous solutions. CBZ was selected due to its relevance as
116 environmental microcontaminant. It is one of the most frequently detected
117 pharmaceuticals in the aquatic environment (Fekadu et al., 2019; Li, 2014; Tran et al.,
118 2018), most possibly as a consequence of being highly recalcitrant to conventional
119 wastewater treatments (Jelic et al., 2011). For these reasons, CBZ has been proposed by

120 several authors as a valid marker of anthropogenic pollution (Bahlmann et al., 2012;
121 Clara et al., 2004). This pharmaceutical (M_w 236.27 g mol⁻¹) is neutral over the range of
122 environmentally relevant pH (pK_a of 13.9, related to the deprotonation of the -NH₂
123 group of CBZ) (Jones et al., 2002) and has a relatively low water solubility (18 mg L⁻¹
124 at 25 °C, with a log K_{ow} of 2.45) (Aga, 2008). The materials produced in this work with
125 the best performance for the adsorption of CBZ, selected after a battery of preliminary
126 tests, were subjected to kinetic and isothermal studies both in ultrapure water and
127 wastewater (final effluent collected at a Sewage Treatment Plant), in order to confirm
128 their adequacy for the target application.

129

130 **2. Material and methods**

131 **2.1. Chemicals**

132 The reagents used for the activation process during the production of AC
133 were potassium hydroxide (KOH; EKA pellets, ≥86%), sodium hydroxide (NaOH;
134 EKA pellets, pure) and phosphoric acid (H₃PO₄; Acros Organics, 85%). For washing
135 the produced materials, hydrochloric acid (HCl; AnalaR NORMAPUR, 37%) was used.
136 CBZ (Sigma-Aldrich, 99%) was the pharmaceutical used for the adsorption
137 experiments, where CBZ aqueous solutions were prepared both in ultrapure water and
138 in wastewater. For the analytical quantification of CBZ by Micellar Electrokinetic
139 Chromatography (as described in section 2.6), all the chemicals used were of analytical
140 grade: sodium dodecylsulphate (SDS, Sigma Aldrich, 99%), hexadimethrine bromide
141 (polybrene, Sigma Aldrich, ≥95%), sodium chloride (José Manuel dos Santos, 99.5%),
142 ethylvanillin (Sigma Aldrich, 99%), sodium tetraborate (Riedel-de-Haën, 99.5%),

143 sodium hydroxide (EKA pellets, pure). The ultrapure water was obtained from a Milli-
144 Q Millipore system (Milli-Q plus 185).

145

146 **2.2. Production of carbon adsorbents**

147 To produce the adsorbent materials, SBG from the brewery Faustino
148 Microcerveja, Lda (Aveiro, Portugal) was used as precursor. In order to evaluate the
149 effect of using SBG arising from different types of fermentation on the properties of the
150 produced materials, two different residues were collected: SBG from the production of
151 Barleywine (BW), a type of beer that has a high fermentation, and SBG from the
152 production of Pilsener (PL), beer that has a low fermentation process. After collection,
153 the SBG was dried at room temperature for several days, followed by a 24 h period at
154 104 °C in an oven, to eliminate the moisture. Then, it was grinded with a blade mill and
155 stored dry until use. The adsorbents were produced by pyrolysis of BW and PL in a
156 furnace muffle (Nüve, series MF 106, Turkey) under inert environment (nitrogen flow),
157 at different temperatures (heating rate of 10 °C min⁻¹) and residence times, and with
158 (AC) or without (*biochar*) a previous activation process, as detailed below. The yield of
159 production (η) of all carbon adsorbents produced was calculated by Eq. (1):

$$160 \quad \eta(\%) = \frac{\text{final mass of carbon adsorbent (g)}}{\text{mass of precursor (g)}} \times 100 \quad (1)$$

161

162 **2.2.1. Preparation of *biochar***

163 The raw SBG was weighed in porcelain crucibles and carbonized at 600 °C and
164 800 °C, using residence times of 60 and 150 min. Accordingly, BW was pyrolyzed
165 under such conditions, resulting in the following materials: BC-BW-600-60, BC-BW-
166 600-150, BC-BW-800-60, and BC-BW-800-150. Preliminary tests carried out with

167 these materials indicated that pyrolysis at 600 °C, without chemical activation, did not
168 result in materials with interesting properties for the adsorptive removal of organic
169 contaminants. For this reason, only the higher temperature (800 °C) was used for PL,
170 i.e., it was treated at 800 °C for 60 min and 150 min, giving the BC-PL-800-60 and BC-
171 PL-800-150 materials. After pyrolysis, the materials were washed with a 0.5 M solution
172 of HCl for the removal of ashes and other inorganic content. For this purpose, for each
173 10 g of material ~200 mL of 0.5 M HCl were added; the materials were immersed in the
174 acid solution for 1 h and subsequently vacuum filtered and washed with distilled water
175 until the washing leachate reached neutral pH (e.g. ~200 mL of distilled water for each
176 10 g of AC activated with alkaline agents or up to a few liters for acid activated
177 materials). Finally, the material was oven dried at 104 °C for 24 h and separated by
178 grain size. The granulometry used in the adsorption tests was below 0.18 mm.

179

180 2.2.2. Preparation of activated carbon

181 Different types of AC were prepared by chemical activation of SBG, followed
182 by carbonization at 800 °C for 150 min. The chemical agents used for activation
183 were KOH, NaOH and H₃PO₄ in a ratio precursor:activating agent of 1:1 (w/w). For the
184 materials activated with KOH and NaOH, the solid activating agent was dissolved in
185 distilled water in a proportion activating agent:water of 3:10 (w/v), whereas for the
186 activation with H₃PO₄, the activating agent was diluted in a ratio activating agent:water
187 of 1:3 (v/v). In both cases, SBG was impregnated for 1 h with the activating agent
188 solution, using an ultrasonic bath. The resulting slurry was then dried at room
189 temperature. Then, the materials were pyrolyzed and subjected to washing and sieving
190 under the same conditions as those described for the *biochar* (section 2.2.1). Six AC

191 materials were obtained: KOH-BW-800-150, NaOH-BW-800-150, H₃PO₄-BW-800-
192 150, KOH-PL-800-150, NaOH-PL-800-150 and H₃PO₄-PL-800-150.

193

194 **2.3. Characterization of precursors and carbon adsorbents**

195 The precursors (PL and BW) and the obtained materials were characterized by
196 the following techniques: total organic carbon, proximate analysis, Fourier transform
197 infrared spectroscopy with attenuated total reflectance (FTIR-ATR), point of zero
198 charge, determination of carbons' functional groups by back-titration, S_{BET} and scanning
199 electron microscopy (SEM). A detailed description of the procedures used can be found
200 in the Supplementary Material (SM).

201

202 **2.4. Batch adsorption experiments**

203 In order to test the adsorptive performance of the produced materials for the
204 removal of CBZ from water, adsorption experiments were made under shaking and
205 batch conditions. In a first analysis of the produced *biochars* and ACs, some
206 preliminary adsorption tests were carried out in order to select the most promising
207 materials that will be subjected to a deeper analysis (kinetic and isothermal studies). For
208 these tests, CBZ solutions with an initial concentration (C_i) of 5 mg L⁻¹ were prepared
209 in ultrapure water. Subsequently, these solutions were placed in polypropylene tubes
210 containing a known mass of adsorbent (varying from 25 to 1000 mg L⁻¹ for *biochars*
211 and 25 to 50 mg L⁻¹ for ACs) and shaken in an overhead shaker (Heidolph, Reax 2) at
212 80 rpm for 24 h and under controlled temperature (25.0 °C ± 0.1 °C). Based on the
213 adsorption percentages resulting from these experiments, the materials with the best
214 adsorptive properties were selected for further studies, as described in sections 2.4.1 and
215 2.4.2.

216 Generally, all studies (preliminary, kinetic and equilibrium) were performed in
217 triplicate. Each experiment included a control (CBZ solution without the adsorbent) that
218 was used as reference for the calculation of adsorption percentages after the contact
219 time between the solution and the material. After stirring under specific conditions,
220 sample aliquots were filtered through 0.22 μm PVDF filters (Whatman) and analyzed by
221 Micellar Electrokinetic Chromatography, in order to determine the remaining
222 pharmaceutical concentration, as described in section 2.6.

223

224 2.4.1. Adsorption kinetics

225 To study the adsorption kinetics of CBZ onto the selected carbons (KOH-BW-
226 800-150 and KOH-PL-800-150), a fixed dose of the carbon adsorbent (mg L^{-1}) was
227 placed in tubes and put in contact with 45 mL of 5 mg L^{-1} of two aqueous solutions of
228 CBZ (prepared in ultrapure water and wastewater, respectively). The concentrations of
229 both KOH-BW-800-150 and KOH-PL-800-150 were 15 mg L^{-1} and 40 mg L^{-1} in
230 ultrapure water and wastewater, respectively. The solutions were shaken for different
231 time intervals between 5 and 240 min for ultrapure water, and 15 and 1860 min for
232 wastewater. A minimum of six time intervals were considered for each system and the
233 dose of carbon material was selected in order to obtain a significant adsorption
234 percentage but, simultaneously, to avoid CBZ removals close to 100% which would
235 difficult the analytical determination of the remaining CBZ concentration. The adsorbed
236 concentration of CBZ onto each AC at time t , q_t (mg g^{-1}), was calculated by Eq. (2). The
237 experimental data were fitted by pseudo-first-order model (Lagergren, 1898) and
238 pseudo-second-order model (Ho et al., 2000), presented in Eqs. (3) and (4), respectively,
239 in order to determine the kinetic parameters of each system.

240 $q_t = \frac{(C_i - C_t)V}{m}$ (2)

241 $q_t = q_e(1 - e^{-k_1 t})$ (3)

242 $q_t = \frac{q_e^2 k_2 t}{1 + k_2 q_e t}$ (4)

243 where C_i (mg L^{-1}) is the initial concentration of pharmaceutical, C_t (mg L^{-1}) is the
244 concentration of pharmaceutical in solution at time t , V (L) is the volume of solution,
245 m is the mass of adsorbent (g), q_e refers to the amount of adsorbate per unit mass of
246 adsorbent at equilibrium (mg g^{-1}), k_1 is the pseudo-first order rate constant (min^{-1}) and
247 k_2 is the pseudo-second order rate constant ($\text{g mg}^{-1} \text{min}^{-1}$). Non-linear fittings were
248 performed using GraphPad Prism, version 5.

249

250 2.4.2. Adsorption equilibrium

251 For the determination of the adsorption isotherms, the experiments were
252 performed using the shaking time needed to attain the equilibrium, as determined in
253 section 2.4.1, and varying the concentration of carbon adsorbents while keeping the
254 initial concentration of the CBZ constant (5 mg L^{-1}). These experiments allow to
255 calculate the adsorption capacity of the materials. Briefly, 50 mL of a 5 mg L^{-1} aqueous
256 solution of CBZ was added at different doses of each carbon. For ultrapure water, the
257 dose of KOH-BW-800-150 and KOH-PL-800-150 varied between $12.5\text{-}30 \text{ mg L}^{-1}$ and
258 $20\text{-}40 \text{ mg L}^{-1}$, respectively; and for wastewater, it varied between $35\text{-}90 \text{ mg L}^{-1}$ and 25-
259 70 mg L^{-1} , respectively. A minimum of six concentrations were considered for each
260 system. The adsorbed concentration of CBZ onto each AC at the
261 equilibrium, q_e (mg g^{-1}), was calculated by Eq. (5). The experimental data were fitted
262 by Langmuir (Langmuir, 1916) and Freundlich (Freundlich, 1906) isotherm models

263 (Eqs. (6) and (7), respectively) in order to determine the equilibrium parameters of the
264 systems. Non-linear fittings were performed using GraphPad Prism, version 5.

$$265 \quad q_e = \frac{(C_i - C_e)V}{m} \quad (5)$$

$$266 \quad q_e = \frac{q_m \times K_L \times C_e}{1 + K_L \times C_e} \quad (6)$$

$$267 \quad q_e = K_F \times C_e^{(1/N)} \quad (7)$$

268 where C_e (mg L^{-1}) is the concentration of CBZ in solution at the equilibrium, q_m is the
269 maximum adsorption capacity of each material towards CBZ (mg g^{-1}), K_L is the
270 Langmuir equilibrium constant (L mg^{-1}), K_F is the Freundlich equilibrium constant (mg
271 $\text{g}^{-1} (\text{L mg}^{-1})^{1/N}$), N are the degrees of non-linearity, and all the other variables are
272 defined as in Eqs. (2), (3) and (4).

273

274 **2.5. Wastewater sampling**

275 Wastewater was collected in June 2019 in a local Sewage Treatment Plant
276 (Aveiro, Portugal) and it corresponds to the final effluent, after the biological treatment,
277 as discharged into receiving waters (~ 3.3 km away from the coast, into the Atlantic
278 Ocean). Immediately after collection in order to remove suspended organic matter, it
279 was filtered through cellulose Supor-450 membrane disc filters $0.45 \mu\text{m}$ with a vacuum
280 system. After filtration, the samples were stored in the dark at $4 \text{ }^\circ\text{C}$ and used within no
281 longer than 15 days. The collected effluent was characterized by measuring conductivity
282 (WTW meter), pH (pH/mV/ $^\circ\text{C}$ meter pHenomenal® pH 1100L, VWR) and dissolved
283 organic carbon content (TOC-VCPH Shimadzu). The pH, conductivity and dissolved
284 organic carbon were 8.42 , 2.78 ms cm^{-1} and $18.0 \pm 0.8 \text{ mg L}^{-1}$, respectively.

285

286 **2.6. Pharmaceutical's quantification**

287 The quantification of CBZ was performed by Micellar Electrokinetic
288 Chromatography using a Beckman P/ACE MDQ instrument (Fullerton, CA, USA),
289 equipped with a UV-Vis detection system, controlled by the software 32 Karat,
290 according to the procedure described by Calisto et al. (Calisto et al., 2011), with minor
291 modifications. Briefly, a coated silica capillary with 30 cm to the detection window was
292 used and the electrophoretic separation was performed at 25 °C and 25 kV, during
293 4.5 min runs. Ethylvanillin was used as internal standard and sodium tetraborate was
294 used to obtain higher repeatability and better peak shape and resolution. Both were
295 spiked to all samples and standard solutions at final concentrations of 3.34 mg L⁻¹ and
296 10 mM, respectively. Detection of CBZ was monitored at 214 nm and the separation
297 buffer consisted of 15 mM of sodium tetraborate and 20 mM of sodium
298 dodecyl sulphate. The calibration curve was determined for a concentration range
299 between 0.25 and 5 mg L⁻¹. All the analyses were performed in triplicate.

300

301 **3. Results and discussion**

302 **3.1. Yield of the adsorbents' production**

303 After the production (pyrolysis and washing) of the adsorbent materials, the
304 production yield was calculated. A considerable difference between the values obtained
305 for the *biochars* and for the ACs was observed. Briefly, the yields obtained were around
306 30 % for all *biochars*; 13 % for BW and PL KOH-ACs; 11 and 4 % for BW and PL
307 NaOH-ACs, respectively; and around 51 % for BW and PL H₃PO₄-ACs. In general, the
308 washing step was an inevitable cause for material losses, due to the removal of the
309 inorganic fraction. The low production yields obtained for the KOH-ACs and NaOH-
310 ACs (in opposition to the ones obtained for *biochars* and H₃PO₄-ACs) can be due to a

311 higher loss of volatile organic matter caused by the reaction with the alkali bases. On
312 the other hand, for H₃PO₄-ACs, the product yield increased comparatively to *biochars*.
313 According to Molina-Sabio et al. (1995), the high yield of H₃PO₄-ACs can be due to the
314 formation of largest structural units by the reaction between this activating agent and the
315 lignocellulosic precursor which do not escape as volatile matter during pyrolysis. This
316 leads to a final material with higher density, most likely due to the generation of
317 phosphate or polyphosphate structures (Hunsom and Autthanit, 2013), contributing to
318 increase the product yield.

319

320 **3.2. Physical and chemical characterization**

321 The results concerning total organic carbon determination are presented in Table
322 S1 of SM. Both precursors present a high value of total organic carbon ($48.5 \pm 0.6\%$
323 and $48.2 \pm 0.2\%$ for BW and PL, respectively) and very low inorganic carbon contents
324 (< limit of detection), corroborating that these residues constitute a promising raw
325 material for the production of carbon adsorbents. Comparing the total organic carbon
326 content values of the carbon adsorbents with those of the precursors, the increase for
327 *biochars* and ACs is clear (~30 %), except for H₃PO₄-BW-800-150 and H₃PO₄-PL-800-
328 150, for which total organic carbon remained similar to the precursor.

329 The thermogravimetric analyses of the raw materials (BW and PL) and the
330 resulting KOH-ACs are depicted in Fig. S1 of SM, while the corresponding proximate
331 analyses, reported on a dry basis, are depicted in Table 1. The results showed that BW
332 and PL have similar characteristics, i.e., low ash contents and high volatile matter and
333 fixed carbon contents. According to Fig. S1, a pronounced thermal decomposition of the
334 precursors began at approximately 200 °C. However, BW and PL have three stages of

335 mass loss during the pyrolysis process, corresponding to derivative thermogravimetric
336 peaks at 84, 295 and 352 °C and 83, 283 and 351 °C, respectively. Initially, the
337 derivative thermogravimetric curve shows a peak (~80 °C) corresponding to the mass
338 loss derived from water evaporation (Mahmood et al., 2017; Oliveira et al., 2018). The
339 major weight loss was observed in the temperature range of 200-500 °C, which is due to
340 the thermal decomposition of the main SBG constituents (cellulose, hemicellulose and
341 lignin) (Mahmood et al., 2017). At ~500 °C the breakdown of lignocellulosic
342 material was finished, and no further weight loss was observed. This indicates that the
343 basic structure of carbon is expected to have been formed at 500 °C, which should be
344 considered as the lowest carbonization temperature for AC production from SBG. The
345 tested pyrolysis temperatures were 600 and 800 °C, since higher temperatures usually
346 translate into a higher development of microporosity, which is advantageous for
347 adsorbents with superior adsorption capacity (Calisto et al., 2014). For KOH-ACs, the
348 volatile matter content is much lower than that of the raw materials. On the other hand,
349 an increase (approximately four times higher) in the fixed carbon content was observed.
350 In fact, the ratio between the volatile matter and fixed carbon percentages for KOH-ACs
351 suffered a substantial decrease compared to the raw materials, indicating an extensive
352 volatile matter release with the increase of the non-volatile carbon fraction, which are
353 two factors that positively contribute to the formation of a carbon rich and highly
354 porous adsorbent (Calisto et al., 2014). The high fixed carbon content is consistent with
355 the total organic carbon determination. Moreover, the low ash content (below 15%) is
356 also in accordance with the low inorganic carbon content of the samples.

357 Regarding FTIR-ATR analyses, the spectra of the BW, PL and of the produced
358 carbon adsorbents are presented in Fig. S2 of SM, allowing to identify the major

359 functional groups. The results show that the precursor materials (both BW and PL) have
360 a much more complex chemical composition than the produced carbon adsorbents. The
361 spectra of BW and PL present several typical bands of cellulose. The bands between
362 2935–2915, 2865–2845 and 2880–2860 cm^{-1} correspond to vibrations of the C–H
363 stretch in asymmetric and symmetric aliphatic chains ($-\text{CH}_2$ and $-\text{CH}_3$, respectively)
364 (Coates, 2000), which may belong to cellulose, lignin or hemicellulose (Fontana et al.,
365 2018). In both cases, these bands disappeared in ACs, however, they are still noted in
366 the BC-BW-800-150 and BC-PL-800-150. The peak at 1743 cm^{-1} , found in spectra of
367 PL, corresponds to the vibration of the stretching of the carbonyl group (C=O) in
368 ketones, ethers, aldehydes and carboxylic acids. In the FTIR spectra of BW and PL-
369 based *biochars* (BC-BW-800-60, BC-BW-800-150, BC-PL-800-60 and BC-PL-800-
370 150), the typical bands of cellulose disappeared. This fact showed that there was a
371 considerable degradation of the main functional groups of BW and PL after pyrolysis,
372 even without activation. Additionally, for spectra of the BW, PL and respective ACs,
373 several peaks are present between 1650 and 1150 cm^{-1} . These peaks can be associated
374 to the cellulosic ethers (C–O–C bonds) ($\sim 1150 \text{ cm}^{-1}$) (Coates, 2000), to the C–O
375 stretching in carbonyl group ($\sim 1238 \text{ cm}^{-1}$) (Coates, 2000), to the C–H bending
376 vibrations ($\sim 1300 \text{ cm}^{-1}$) (Fontana et al., 2018; Jaria et al., 2017), and to the carbonyl
377 group in aromatic rings ($\sim 1641 \text{ cm}^{-1}$) (Calisto et al., 2014; Coates, 2000) found in lignin
378 (Fontana et al., 2018). The groups identified in the FTIR spectra of the BW and PL are
379 in agreement with the brewing waste composition, which is rich in cellulose
380 hemicellulose, lignin and proteins (Olszewski et al., 2019; Wierzba et al., 2019).

381 The point of zero charge (Table 2 and Fig. S3 of SM) was determined in order to
382 know the net charge of the ACs. The concentrations of some functional groups, namely

383 carboxyl and total basic groups, were obtained by back titrations (Table 2). Low point
384 of zero charge is directly connected with the presence of high concentrations of the
385 carboxyl groups; on the other hand, higher point of zero charge is linked to a higher
386 concentration of total basic groups and lower concentration of carboxyl groups. The
387 point of zero charge determined for KOH-BW-800-150 and KOH-PL-800-150 is
388 neutral or slightly basic, respectively, which is in line with the very similar
389 concentrations obtained for the two functional groups for both materials.

390 For the study of the textural features of the materials, nitrogen adsorption
391 isotherms and SEM were used as characterization techniques. The results of S_{BET} and
392 the textural characterization of all the produced carbon adsorbents are presented in
393 Table 3. PL-based carbons presented slightly higher S_{BET} compared with BW-based
394 carbons produced under the same conditions. This fact may be explained by the relative
395 higher content of volatile matter in PL in comparison with BW. KOH-BW-800-150 and
396 KOH-PL-800-150 were the materials with the highest S_{BET} , 1090 and 1120 $\text{m}^2 \text{g}^{-1}$,
397 respectively. On the other hand, the ACs obtained with NaOH and H_3PO_4 chemical
398 activation resulted in much lower S_{BET} , more comparable with the values obtained for
399 the *biochars* than with the KOH-based ACs. The same conclusion is valid for total pore
400 volume (V_p) and micropore volume (W_0) values, which will certainly influence the
401 adsorptive capacity of these materials. This comparison is particularly interesting in the
402 case of the materials resulting from KOH and NaOH chemical activation: the activating
403 agents are of similar nature, both alkali hydroxides, but the results are drastically
404 different for the two alkali metals, indicating that potassium has a determinant influence
405 in the development of the microporosity.

406 A comparison of the S_{BET} values obtained by other literature studies using
407 precursors with similar nature reveals that the results presented in this manuscript are
408 quite interesting. There are some works that use SGB in its raw form, as that described
409 by Fontana et al. (Fontana et al., 2016), who only dried, crushed and sieved the raw
410 material, and they obtained a S_{BET} of $0.8246 \text{ m}^2 \text{ g}^{-1}$. In what concerns materials resulting
411 from chemical activation, most authors initially carbonize the previously dried SBG and
412 then activate the resultant carbon material, adopting a two-step activation instead of the
413 one-step procedure applied in the present manuscript. The study of Olajire et al. (2017)
414 is an example of such cases, where dry SBG was carbonized at $300 \text{ }^\circ\text{C}$ during 30
415 minutes and subsequently activated with H_3PO_4 and subjected to a second carbonization
416 at $300 \text{ }^\circ\text{C}$ during 1h. The resultant carbon presented a S_{BET} of $412 \text{ m}^2 \text{ g}^{-1}$ (Olajire et al.,
417 2017). Also, a comparison of the materials described in this study with some
418 commercially available ACs show that KOH-BW-800-150 and KOH-PL-800-150
419 presented higher S_{BET} . For example the commercial AC, PULSORB FG4 (PBFG4) and
420 Norit (SAE SUPER 8003.6) (applied by Calisto et al. (Calisto et al., 2014) and Silva et
421 al. (Silva et al., 2019), respectively) have a S_{BET} of 848 and $996 \text{ m}^2 \text{ g}^{-1}$, respectively,
422 indicating that the produced materials have very promising properties to be used as
423 adsorbents.

424 Fig. 1 shows the SEM images of both precursors and some examples of BW and
425 PL-based carbons. The images show a gradual difference between the surface
426 morphology of the precursors, the *biochars* and of the KOH-ACs. In comparison to
427 ACs, the structure of *biochars* is more homogeneous, with some degree of destruction
428 of the original structure and a few pores can be observed (as confirmed by S_{BET}
429 analysis). On the other hand, the structure of the KOH-AC is a much rougher surface

430 (particularly, for PL-materials) with a well-developed porosity. The highly porous
431 structure is in accordance with a higher surface area, as can be confirmed by the results
432 of S_{BET} , V_p and W_0 (Table 3). Other SEM images of the *biochars* and KOH-AC are
433 presented in Figs. S4 and S5 of SM, respectively, at different magnifications.

434

435 **3.3. Batch adsorption experiments**

436 Preliminary tests were performed to evaluate the adsorptive removal of CBZ
437 from water by all the produced carbons, allowing to identify the most promising
438 materials. For the *biochars*, a considerable range of carbon dosages (between 25 and
439 1000 mg L⁻¹) was tested. The results showed a negligible CBZ adsorption, even at
440 materials' dose as high as 1000 mg L⁻¹ (data not shown). This performance is in
441 accordance with the very low S_{BET} obtained for the non-activated carbons. Therefore,
442 kinetic and equilibrium studies were not performed with *biochars*.

443 On the other hand, the ACs revealed much more interesting results, even at
444 much lower carbon doses (25 and 50 mg L⁻¹) as evidenced by the data depicted in Table
445 S2 of SM. The ACs with the best adsorptive performance to remove CBZ ($C_i = 5$ mg L⁻¹)
446 from aqueous solutions were KOH-BW-800-150 and KOH-PL-800-150, with
447 adsorption percentages of $88 \pm 11\%$ and $85 \pm 7\%$, respectively, using only 25 mg L⁻¹ of
448 material. The others ACs were not able to satisfactorily adsorb CBZ at the tested doses,
449 with removal percentages below $15 \pm 6\%$, using 50 mg L⁻¹ of material. Better removal
450 percentages for the KOH-ACs are certainly related with their S_{BET} , V_p and W_0 , which are
451 much higher than those obtained for NaOH-ACs and H₃PO₄-ACs (Table 3). Based on
452 these results, the two KOH-ACs (KOH-BW-800-150 and KOH-PL-800-150) were
453 selected to perform kinetic and equilibrium studies. For this purpose, both ultrapure

454 water and wastewater were used as test matrices, in order to evaluate the adsorptive
455 behavior of the materials under more realistic and representative conditions.

456

457 3.3.1. Adsorption kinetics

458 The amount of CBZ adsorbed onto KOH-BW-800-150 and KOH-PL-800-150 at
459 time t (q_t , mg g^{-1}) versus time, as well as the fittings of the experimental data to pseudo-
460 first and second orders kinetic models (Eqs. (3) and (4), respectively) are represented in
461 Fig. 2. The fitting parameters are summarized in Table 4. Generally, the pseudo-second-
462 order model was the model that best fitted the experimental data, with determination
463 coefficients (r^2) ranging from 0.974 to 0.985 (except for KOH-BW-800-150 in ultrapure
464 water). The adequacy of the pseudo-second-order model to describe the adsorption of
465 CBZ onto carbon adsorbents was in line with the results previously reported in several
466 literature studies, where this model was the one presenting the most satisfactory fittings
467 to the experimental data (Calisto et al., 2017, 2015; Chen et al., 2017; Oliveira et al.,
468 2018; Silva et al., 2019; To et al., 2017).

469 Considering the adsorption of CBZ onto KOH-BW-800-150 and KOH-PL-800-
470 150, it can be verified that the observed adsorption rates (k_2) determined by the pseudo-
471 second-order model indicated that no major differences can be found for the adsorption
472 kinetics for both materials and both matrices. All the systems attained adsorption
473 equilibrium after 120 to 240 min of contact between the adsorbent and CBZ. Overall,
474 and considering that equilibrium is quickly reached, both SBG-based carbons are
475 kinetically adequate for wastewater treatment, combining quick kinetics with no
476 significant matrix interferences (that could have been possibly observed due to the

477 compositional complexity of the Sewage Treatment Plant's effluent) in the time needed
478 to attain equilibrium.

479

480 3.3.2. Adsorption equilibrium

481 The adsorption isotherms, represented as the amount of CBZ adsorbed onto
482 KOH-BW-800-150 and KOH-PL-800-150 at equilibrium (q_e , mg g⁻¹) *versus* the amount
483 of pharmaceutical remaining in solution (C_e , mg L⁻¹), are shown in Fig. 3. The fitting
484 parameters obtained for the experimental data using Langmuir and Freundlich isotherm
485 models (Eqs. (6) and (7), respectively) are summarized in Table 4. The Langmuir-
486 Freundlich equilibrium model (Sips, 1948) has also been tested for fitting the
487 experimental data. However, the determination of the Langmuir-Freundlich adsorption
488 parameters was ambiguous for all systems, and thus it was not considered in this
489 discussion.

490 According to the results obtained for the r^2 , ranging from 0.953 to 0.983, the
491 equilibrium experimental data are satisfactorily described by the Langmuir model, for
492 both matrices and materials. As evidenced in Fig. 3 and confirmed by the adsorption
493 parameters depicted in Table 4, it was possible to conclude that the Langmuir maximum
494 adsorption capacity (q_m) for KOH-BW-800-150 and KOH-PL-800-150, was
495 significantly higher in ultrapure water than in wastewater. The q_m in wastewater
496 decreased ~70 and ~60% for KOH-BW-800-150 and KOH-PL-800-150, respectively.
497 This can be due to the complex chemical composition of the wastewater, which contains
498 organic and inorganic components, such as dissolved organic matter, that can compete
499 for the adsorption sites of the carbons and, consequently, hamper the access to the pores
500 of the adsorbents (Oliveira et al., 2018; Silva et al., 2019). These results reinforce that,
501 despite the relevance of a first evaluation of the adsorptive capacity of the materials in

502 ultrapure water, tests using real wastewater are of utmost importance to predict the
503 behavior of the adsorbents under conditions as close as possible to their real application.

504 A comparison between KOH-BW-800-150 and KOH-PL-800-150 reveals that
505 these two materials have a similar q_m (190 ± 27 and 178 ± 10 , respectively), in ultrapure
506 water. In wastewater the q_m was slightly lower for KOH-BW-800-150 than for KOH-
507 PL-800-150 (57.4 ± 1.6 and 76.0 ± 1.5 , respectively). Still, the performance of the
508 materials is very similar with no major differences between them, highlighting that SBG
509 resulting from different fermentation levels do not result in adsorbents materials with
510 significantly distinct adsorptive properties for the systems considered in the present
511 study.

512 The removal of CBZ from both ultrapure water and wastewater through
513 adsorption onto commercial or waste-based carbon adsorbents has been addressed in the
514 literature by several authors. Table 5 presents some examples of relevant studies from
515 the last 5 years, allowing for a comparative evaluation of the performance of the
516 materials depicted in the present study. Along with the maximum adsorption capacity
517 towards CBZ, S_{BET} of the materials was also presented as it is considered a key property
518 of the adsorbents. The results here obtained are comparable to the performances
519 observed for commercial ACs, which attained q_m between 116 mg g^{-1} (Calisto et al.,
520 2015) and 242 mg g^{-1} (Delgado et al., 2019) in ultrapure pure or distilled water. This is a
521 good indication of the satisfactory removal efficiencies of the materials derived from
522 SBG chemical activation and pyrolysis. When compared with other waste-based
523 adsorbents, *biochars* produced by carbonization with no activation agents have
524 significantly lower performances (Calisto et al., 2017; Nielsen et al., 2015), as it was
525 also verified for the *biochars* produced from SBG, corroborating the need of such

526 activation procedures to attain efficiencies comparable to commercially available
527 options. On the other hand, ACs produced from industrial or agricultural wastes present
528 significantly higher performances than *biochars* and similar to the results obtained for
529 AC produced from SBG (up to 190 mg g⁻¹), varying from 93 mg g⁻¹ (Oliveira et al.,
530 2018) to 335 mg g⁻¹ (Torrellas et al., 2015). While the evaluation of the materials'
531 adsorptive capacity in ultrapure or distilled water is always considered in the literature,
532 fewer works were carried out in real matrices, namely wastewater. In these cases, and
533 considering CBZ in particular, some studies reported that the adsorptive removal
534 remained almost unchanged (Silva et al., 2019) while others observed a significant
535 decrease in the ability to remove the target pollutant (Oliveira et al., 2018), as verified
536 for the AC described in the present work. In this context, further research needs to be
537 done to improve the adsorptive performance of the adsorbent materials at conditions
538 representative of the target application, where the competition with dissolved organic
539 matter and other organic and inorganic compounds could be determinant. The
540 modification of the adsorbent surface by chemical functionalization could be a possible
541 way to improve the affinity of the materials towards specific pharmaceuticals.

542 Overall, considering the large-scale production all over the world and the
543 sustainable nature of the precursor used in the production of adsorbents, the results
544 presented in this study indicate that SBG is a viable AC precursor that might be
545 successfully applied to the removal of pharmaceuticals from water. Nevertheless, it
546 should be highlighted that the sustainability of the whole process can be hampered by
547 the use of high temperatures and pyrolysis times combined with high proportions of
548 activating agents, which are required for obtaining materials with adequate properties
549 for increased adsorptive performances. In this sense, further research should be carried

550 out to investigate the conversion of SBG into AC using milder conditions by applying,
551 for instance, alternative heating technologies, such as microwave-induced pyrolysis.
552 Moreover, the produced adsorbents are in powdered form, which might hinder their
553 affordable applicability in Sewage Treatment Plants due to the need of introducing an
554 additional step aimed at separating the treated aqueous phase from the powdered AC.
555 This might be overcome by (i) testing the introduction of magnetic properties in the
556 produced AC, and (ii) testing the performance of SBG-derived granular materials. In
557 fact, the applied production process allows to obtain higher particle sizes (granular AC)
558 without the need of any extra step (such as the addition of agglomeration agents).

559

560 **4. Conclusions**

561 The chemical activation of SBG was fundamental to obtain high-efficiency
562 adsorbents, being KOH-ACs the materials with the most interesting physicochemical
563 characteristics and the best adsorptive performance towards CBZ. Moreover, using as
564 precursor SBG from different types of fermentation does not influence the adsorbents'
565 properties. Adsorption studies in Sewage Treatment Plant's wastewater allowed to
566 verify a decrease in the performance of the materials, in comparison to ultrapure water,
567 highlighting the importance of using realistic matrices as model systems. This study
568 represents a step forward in the utilization of SBG for ACs production, enabling its
569 application to the effective adsorption of pharmaceuticals.

570

571 **Supplementary Materials**

572 E-supplementary data of this work can be found in online version of the paper.

573

574 **Acknowledgments**

575 Thanks are due for the financial support to CESAM (UID/AMB/50017/2019), to
576 FCT/MEC through national funds, and the co-funding by the FEDER, within the
577 PT2020 Partnership Agreement and Compete 2020. Vânia Calisto is thankful to FCT
578 for the Scientific Employment Stimulus Program (CEECIND/00007/2017), while Maria
579 V. Gil acknowledges support from a Ramón y Cajal grant (RYC-2017-21937) of the
580 Spanish government, co-financed by the European Social Fund (ESF). The authors
581 would like to thank Valdemar Esteves, Marta Otero and Guilaine Jaria for the helpful
582 scientific discussions. Milton Fontes and workers of Aveiro's Sewage Treatment Plant
583 (Águas do Centro Litoral) are gratefully acknowledged for assistance on the effluent
584 sampling campaigns. The authors also thank *Faustino Microcervejeira, Lda.* (Aveiro,
585 Portugal) and its head brewer Gonçalo Faustino for kindly providing the brewing
586 residues used in this work.

587

588 **References**

- 589 Aga, D.S., 2008. Fate of pharmaceuticals in the environment and in water treatment
590 systems.
- 591 Azargohar, R., Dalai, A.K., 2008. Steam and KOH activation of biochar: Experimental
592 and modeling studies. *Microporous Mesoporous Mater.* 110, 413–421.
593 doi:10.1016/j.micromeso.2007.06.047
- 594 Bahlmann, A., Carvalho, J.J., Weller, M.G., Panne, U., Schneider, R.J., 2012.
595 Immunoassays as high-throughput tools: Monitoring spatial and temporal
596 variations of carbamazepine, caffeine and cetirizine in surface and wastewaters.
597 *Chemosphere* 89, 1278–1286. doi:10.1016/j.chemosphere.2012.05.020

598 Barrozo, M.A.S., Borel, L.D., Lira, T.S., Ataíde, C.H., 2019. Fluid dynamics analysis
599 and pyrolysis of brewer's spent grain in a spouted bed reactor. *Particuology* 42,
600 199–207. doi:10.1016/j.partic.2018.06.001

601 Borel, L.D., Lira, T.S., Ribeiro, J.A., Ataíde, C.H., Barrozo, M.A.S., 2018. Pyrolysis of
602 brewer's spent grain: Kinetic study and products identification. *Ind. Crops Prod.*
603 121, 388–395. doi:10.1016/j.indcrop.2018.05.051

604 Calisto, V., Domingues, M.R.M., Erny, G.L., Esteves, V.I., 2011. Direct
605 photodegradation of carbamazepine followed by micellar electrokinetic
606 chromatography and mass spectrometry. *Water Res.* 45, 1095–1104.
607 doi:10.1016/j.watres.2010.10.037

608 Calisto, V., Ferreira, C.I.A., Oliveira, J.A.B.P., Otero, M., Esteves, V.I., 2015.
609 Adsorptive removal of pharmaceuticals from water by commercial and waste-
610 based carbons. *J. Environ. Manage.* 152. doi:10.1016/j.jenvman.2015.01.019

611 Calisto, V., Ferreira, C.I.A., Santos, S.M., Gil, M.V., Otero, M., Esteves, V.I., 2014.
612 Production of adsorbents by pyrolysis of paper mill sludge and application on the
613 removal of citalopram from water. *Bioresour. Technol.* 166, 335–344.
614 doi:http://dx.doi.org/10.1016/j.biortech.2014.05.047

615 Calisto, V., Jaria, G., Silva, C.P., Ferreira, C.I.A., Otero, M., Esteves, V.I., 2017. Single
616 and multi-component adsorption of psychiatric pharmaceuticals onto alternative
617 and commercial carbons. *J. Environ. Manage.* 192, 15–24.

618 Chen, D., Xie, S., Chen, C., Quan, H., Hua, L., Luo, X., Guo, L., 2017. Activated
619 biochar derived from pomelo peel as a high-capacity sorbent for removal of
620 carbamazepine from aqueous solution. *RSC Adv.* 7, 54969–54979.
621 doi:10.1039/C7RA10805B

- 622 Clara, M., Strenn, B., Kreuzinger, N., 2004. Carbamazepine as a possible anthropogenic
623 marker in the aquatic environment: investigations on the behaviour of
624 carbamazepine in wastewater treatment and during groundwater infiltration. *Water*
625 *Res.* 38, 947–954.
- 626 Coates, J., 2000. Interpretation of Infrared Spectra - A Practical Approach, in: Meyers,
627 R.A. (Ed.), *Encyclopedia of Analytical Chemistry*. John Wiley & Sons Ltd,
628 Chichester, pp. 10815–10837.
- 629 Delgado, N., Capparelli, A., Navarro, A., Marino, D., 2019. Pharmaceutical emerging
630 pollutants removal from water using powdered activated carbon: Study of kinetics
631 and adsorption equilibrium. *J. Environ. Manage.* 236, 301–308.
632 doi:10.1016/J.JENVMAN.2019.01.116
- 633 Fekadu, S., Alemayehu, E., Dewil, R., Van der Bruggen, B., 2019. Pharmaceuticals in
634 freshwater aquatic environments: A comparison of the African and European
635 challenge. *Sci. Total Environ.* 654, 324–337.
636 doi:10.1016/J.SCITOTENV.2018.11.072
- 637 Ferraz, A.I., Tavares, M.T., Teixeira, J.A., 2005. Sorption of Cr (III) from aqueous
638 solutions by spent brewery grain. *CHEMPOR 2005 - 9th Int. Chem. Eng. Conf.*
639 s.n.
- 640 Fontana, I.B., Peterson, M., Cechinel, M.A.P., 2018. Application of brewing waste as
641 biosorbent for the removal of metallic ions present in groundwater and surface
642 waters from coal regions. *J. Environ. Chem. Eng.* 6, 660–670.
643 doi:10.1016/J.JECE.2018.01.005
- 644 Fontana, K.B., Chaves, E.S., Sanchez, J.D.S., Watanabe, E.R.L.R., Pietrobelli,
645 J.M.T.A., Lenzi, G.G., 2016. Textile dye removal from aqueous solutions by malt

646 bagasse: Isotherm, kinetic and thermodynamic studies. *Ecotoxicol. Environ. Saf.*
647 124, 329–336. doi:10.1016/j.ecoenv.2015.11.012

648 Freundlich, H., 1906. Over the adsorption in solution. *J. Phys. Chem.* 18, 385–470.

649 Gonçalves, G. da C., Nakamura, P.K., Furtado, D.F., Veit, M.T., 2017. Utilization of
650 brewery residues to produces granular activated carbon and bio-oil. *J. Clean. Prod.*
651 168, 908–916. doi:10.1016/J.JCLEPRO.2017.09.089

652 Ho, Y.S., McKay, G., Wase, D.A.J., Forster, C.F., 2000. Study of the sorption of
653 divalent metal ions on to peat. *Adsorpt. Sci. Technol.* 18, 639–650.
654 doi:10.1260/0263617001493693

655 Hunsom, M., Autthanit, C., 2013. Adsorptive purification of crude glycerol by sewage
656 sludge-derived activated carbon prepared by chemical activation with H₃PO₄ ,
657 K₂CO₃ and KOH. *Chem. Eng. J.* 229, 334–343. doi:10.1016/j.cej.2013.05.120

658 Jaria, G., Calisto, V., Gil, M.V., Otero, M., Esteves, V.I., 2015. Removal of fluoxetine
659 from water by adsorbent materials produced from paper mill sludge. *J. Colloid*
660 *Interface Sci.* 448, 32–40. doi:http://dx.doi.org/10.1016/j.jcis.2015.02.002

661 Jaria, G., Calisto, V., Silva, C.P., Gil, M.V., Otero, M., Esteves, V.I., 2019. Obtaining
662 granular activated carbon from paper mill sludge – A challenge for application in
663 the removal of pharmaceuticals from wastewater. *Sci. Total Environ.* 653, 393–
664 400. doi:10.1016/J.SCITOTENV.2018.10.346

665 Jaria, G., Silva, C.P., Ferreira, C.I.A., Otero, M., Calisto, V., 2017. Sludge from paper
666 mill effluent treatment as raw material to produce carbon adsorbents: An
667 alternative waste management strategy. *J. Environ. Manage.* 188, 203–211.

668 Jelic, A., Gros, M., Ginebreda, A., Cespedes-Sánchez, R., Ventura, F., Petrovic, M.,
669 Barcelo, D., 2011. Occurrence, partition and removal of pharmaceuticals in sewage

670 water and sludge during wastewater treatment. *Water Res.* 45, 1165–1176.
671 doi:10.1016/j.watres.2010.11.010

672 Jones, O.A., Voulvoulis, N., Lester, J.N., 2002. Aquatic environmental assessment of
673 the top 25 English prescription pharmaceuticals. *Water Res.* 36, 5013–5022.

674 Lagergren, S., 1898. About the Theory of So-called Adsorption of Soluble Substances.
675 *K. Sven. Vetenskapsakademiens* 24, 1–39.

676 Langmuir, I., 1916. The constitution and fundamental properties of solids and liquids. *J.*
677 *Am. Chem. Soc.* 38, 2221–2295. Doi:10.1021/ja02268a002

678 Li, W.C.C., 2014. Occurrence, sources, and fate of pharmaceuticals in aquatic
679 environment and soil. *Environ. Pollut.* 187, 193–201.
680 doi:10.1016/j.envpol.2014.01.015

681 Mahmood, T., Ali, R., Naeem, A., Hamayun, M., Aslam, M., 2017. Potential of used
682 *Camellia sinensis* leaves as precursor for activated carbon preparation by chemical
683 activation with H₃PO₄; optimization using response surface methodology. *Process*
684 *Saf. Environ. Prot.* 109, 548–563. doi:10.1016/j.psep.2017.04.024

685 Molina-Sabio, M., Rodríguez-Reinoso, F., Caturla, F., Sellés, M.J., 1995. Porosity in
686 granular carbons activated with phosphoric acid. *Carbon N. Y.* 33, 1105–1113.
687 doi:https://doi.org/10.1016/0008-6223(95)00059-M

688 Nielsen, L., Zhang, P., Bandosz, T.J., 2015. Adsorption of carbamazepine on
689 sludge/fish waste derived adsorbents: Effect of surface chemistry and texture.
690 *Chem. Eng. J.* 267, 170–181. doi:10.1016/J.CEJ.2014.12.113

691 Olajire, A., Abidemi, J., Lateef, A., Benson, N.U., 2017. Adsorptive desulphurization of
692 model oil by Ag nanoparticles-modified activated carbon prepared from brewer's
693 spent grains. *J. Environ. Chem. Eng.* 5, 147–159. doi:10.1016/j.jece.2016.11.033

694 Oliveira, G., Calisto, V., Santos, S.M., Otero, M., Esteves, V.I., 2018. Paper pulp-based
695 adsorbents for the removal of pharmaceuticals from wastewater: A novel approach
696 towards diversification 631–632, 1018–1028.

697 Olszewski, M.P., Arauzo, P.J., Wądrzyk, M., Kruse, A., 2019. Py-GC-MS of
698 hydrochars produced from brewer's spent grains. *J. Anal. Appl. Pyrolysis* 140,
699 255–263. doi:10.1016/j.jaap.2019.04.002

700 Silva, C.P., Jaria, G., Otero, M., Esteves, V.I., Calisto, V., 2019. Adsorption of
701 pharmaceuticals from biologically treated municipal wastewater using paper mill
702 sludge-based activated carbon. *Environ. Sci. Pollut. Res.* 26, 13173–13184.
703 doi:10.1007/s11356-019-04823-w

704 Silva, J.P., Sousa, S., Rodrigues, J., Antunes, H., Porter, J., Gonçalves, I., Ferreira-Dias,
705 S., 2004. Adsorption of acid orange 7 dye in aqueous solutions by spent brewery
706 grains. *Sep. Purif. Technol.* 40, 309–315. doi:10.1016/j.seppur.2004.03.010

707 Sips, R., 1948. On the structure of a catalyst surface. *J. Chem. Phys.* 16, 490–495.
708 doi:10.1063/1.1746922

709 To, M.-H., Hadi, P., Hui, C.-W., Lin, C.S.K., McKay, G., 2017. Mechanistic study of
710 atenolol, acebutolol and carbamazepine adsorption on waste biomass derived
711 activated carbon. *J. Mol. Liq.* 241, 386–398. doi:10.1016/J.MOLLIQ.2017.05.037

712 Torrellas, S.Á., García Lovera, R., Escalona, N., Sepúlveda, C., Sotelo, J.L., García, J.,
713 2015. Chemical-activated carbons from peach stones for the adsorption of
714 emerging contaminants in aqueous solutions. *Chem. Eng. J.* 279, 788–798.

715 Tran, N.H., Reinhard, M., Gin, K.Y.-H., 2018. Occurrence and fate of emerging
716 contaminants in municipal wastewater treatment plants from different geographical
717 regions-a review. *Water Res.* 133, 182–207. doi:10.1016/J.WATRES.2017.12.029

- 718 Vanreppelen, K., Vanderheyden, S., Kuppens, T., Schreurs, S., Yperman, J., Carleer, R.,
719 2014. Activated carbon from pyrolysis of brewer's spent grain: Production and
720 adsorption properties. *Waste Manag. Res.* 32, 634–645.
721 doi:10.1177/0734242X14538306
- 722 Wierzba, S., Andrzej, K., 2019. Heavy metal sorption in biosorbents - Using spent grain
723 from the brewing industry. *J. Clean. Prod.* 225, 112–120.
724 doi:10.1016/j.jclepro.2019.03.286
- 725 Wierzba, S., Rajfur, M., Nabrdalik, M., Kłos, A., 2019. Assessment of the influence of
726 counter ions on biosorption of copper cations in brewer's spent grain - Waste
727 product generated during beer brewing process. *Microchem. J.* 145, 196–203.
728 doi:10.1016/j.microc.2018.10.040
729

Table 1. Proximate analyses for precursors (BW and PL) and activated carbons produced by chemical activation with KOH (KOH-BW-800-150 and KOH-PL-800-150)

Material	Moisture	Volatile matter (VM)	Fixed carbon (FC)	Ash	VM/FC
		(wt%, dry basis)			
BW	3.34	74.08	21.95	3.97	3.38
PL	2.86	75.75	19.30	4.95	3.93
KOH-BW-800-150	24.71	12.43	83.12	4.45	0.15
KOH-PL-800-150	22.90	8.24	78.00	13.76	0.11

Table 2. Point of zero charge and amount of carboxyl and total basic functional groups of KOH-BW-800-150 and KOH-PL-800-150 determined by back titration

Material	Functional groups (mmol g ⁻¹)		Point of zero charge
	Carboxylic acids	Basic groups (Total)	
KOH-BW-800-150	2.27	2.29	6.9
KOH-PL-800-150	2.28	2.56	8.0

Table 3. Textural characterization of all the produced carbon adsorbents – specific surface area (S_{BET}); total pore volume (V_p); micropore volume (W_0); and average micropore width (L).

Material	S_{BET} (m ² g ⁻¹)	V_p (cm ³ g ⁻¹)	Dubinin-Astakhov (DA)	
			W_0 (cm ³ g ⁻¹)	L (nm)
BC-BW-800-60	3	0.01	0.001	1.79
BC-BW-800-150	3	0.01	0.001	1.77
KOH-BW-800-150	1090	0.55	0.44	1.48
NaOH-BW-800-150	18	0.02	0.01	1.95
H ₃ PO ₄ -BW-800-150	14	0.02	0.01	1.86
BC-PL-800-60	4	0.02	0.002	1.91
BC-PL-800-150	5	0.02	0.002	1.82
KOH-PL-800-150	1120	0.60	0.46	1.49
NaOH-PL-800-150	267	0.54	0.12	1.73
H ₃ PO ₄ -PL-800-150	29	0.05	0.02	2.04

Table 4. Fitting parameters of pseudo-first and pseudo-second order kinetic models, and of Langmuir and Freundlich equilibrium models, to the experimental data

		Ultrapure water		Wastewater	
		KOH-BW-800-150	KOH-PL-800-150	KOH-BW-800-150	KOH-PL-800-150
<i>Kinetic models</i>					
Pseudo 1 st order	q_e (mg g ⁻¹)	179 ± 4	182 ± 9	45 ± 3	59 ± 4
	k_1 (min ⁻¹)	0.066 ± 0.006	0.09 ± 0.02	0.024 ± 0.005	0.037 ± 0.009
	r^2	0.993	0.959	0.948	0.933
	n^*	7	7	7	7
Pseudo 2 nd order	q_e (mg g ⁻¹)	199 ± 11	201 ± 7	51 ± 3	64 ± 2
	k_2 (mg g ⁻¹ min)	0.0004 ± 0.0001	0.0006 ± 0.0001	0.0005 ± 0.0001	0.0009 ± 0.0002
	r^2	0.974	0.985	0.979	0.974
	n^*	7	7	7	7
<i>Equilibrium adsorption models</i>					
Langmuir	q_m (mg g ⁻¹)	190 ± 27	178 ± 10	57.4 ± 1.6	76.0 ± 1.5
	K_L (L mg ⁻¹)	3 ± 2	6 ± 2	36 ± 21	60 ± 25
	r^2	0.953	0.966	0.973	0.983
	n^*	6	9	9	9
Freundlich	K_F	144 ± 12	151 ± 4	55.0 ± 1.3	73.4 ± 1.4
	(mg g ⁻¹ (mg L ⁻¹) ^{-N})				
	N	7 ± 5	5.3 ± 1.6	32 ± 25	25 ± 12
	r^2	0.944	0.959	0.966	0.979
n^*	6	9	9	9	

* n is the number of data points used in the fitting.

Table 5. Examples of literature studies reporting the adsorptive removal of carbamazepine using commercial or waste-based carbon adsorbents

Adsorbent	S _{BET} (m ² g ⁻¹)	Equilibrium experimental conditions ¹	Maximum adsorption capacity ² (mg g ⁻¹)	Reference
Commercial AC (PBF4)	848	T = 25 °C; C ₀ = 5 mg L ⁻¹	116 (ultrapure water)	(Calisto et al. 2015)
Comercial AC (Norit)	996	T = 25 °C; C ₀ = 5 mg L ⁻¹	174 (ultrapure water); 160 (wastewater, pH 7.7 - 7.9)	(Silva et al. 2019)
Commercial AC from vegetable origin	1328	T = 25 °C; C ₀ = 10 - 40 mg L ⁻¹	242 (distilled water, pH ~6)	(Delgado et al. 2019)
Biochar from paper mill sludge	414	T = 25 °C; C ₀ = 5 mg L ⁻¹	17.4 (ultrapure water, converted from μmol g ⁻¹)	(Calisto et al. 2017)
Carbonized sewage sludge+fish waste	34 - 101	T = 30 °C; C ₀ = 1 – 100 mg L ⁻¹	4.9 – 37.2 (Sips isotherm)	(Nielsen et al. 2015)
AC from bleached paper pulp	768 - 965	T = 25 °C; C ₀ = 5 mg L ⁻¹	57 - 93 (ultrapure water); 29.9 - 80 (wastewater, pH 7.8)	(Oliveira et al. 2018)
AC from paper mill sludge	1627	T = 25 °C; C ₀ = 5 mg L ⁻¹	212 (ultrapure water); 209 (wastewater, pH 7.7 - 7.9)	(Silva et al. 2019)
AC from palm kernel shell	711.5	T = 25 °C; C ₀ = 100 – 250 mg L ⁻¹	208 (ultrapure water, pH 7, converted from mmol g ⁻¹)	(To et al. 2017)
AC from peach stones	959 - 1216	T = 30 °C; C ₀ = 100 mg L ⁻¹	335 (ultrapure water)	(Torrellas et al. 2015)
AC from pomelo peel	198.0 – 904.1	T = 25 °C; C ₀ = 10 – 100 mg L ⁻¹	80.64 - 286.5 (ultrapure water)	(Chen et al. 2017)
AC from spent brewery grains	1090-1120	T = 25 °C; C ₀ = 5 mg L ⁻¹	178 - 190 (ultrapure water); 57.4 – 76.0 (wastewater, pH 8.4)	This study

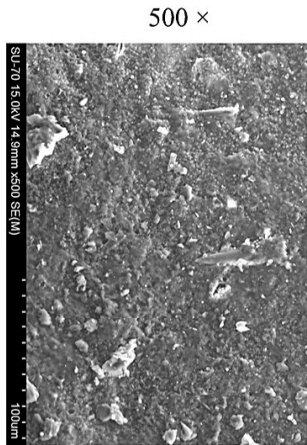
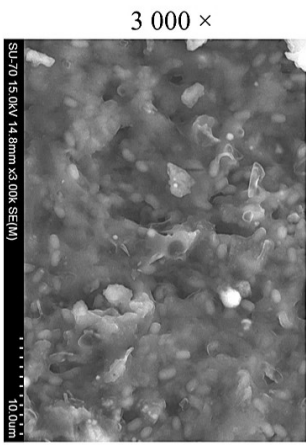
¹ C₀ – carbamazepine initial concentration

² Maximum adsorption capacity determined by fitting the experimental data with the Langmuir isotherm model, unless stated otherwise

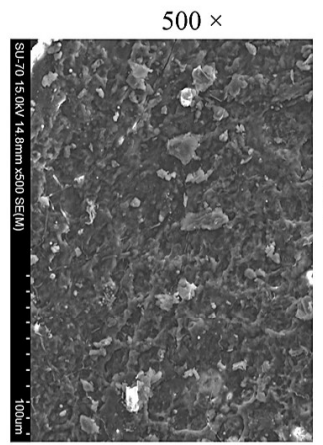
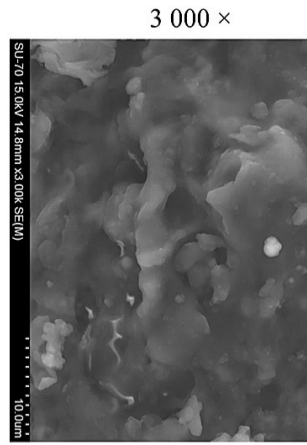
Fig. 1. SEM images of precursors (BW, PL), *biochars* (BC-BW-800-150, BC-PL-800-150) and AC (KOH-BW-800-150 and KOH-PL-800-150) at different magnifications

Fig. 2. Kinetic fittings for experimental data for KOH-BW-800-150 in a) ultrapure water and b) wastewater; and for KOH-PL-800-150 in c) ultrapure water and d) wastewater. The results were fitted to pseudo-first (solid lines) and pseudo-second (dashed lines) order kinetic models. Each point (\pm standard deviation) is the average of three replicates. Note that x and y -axis scales are not the same in all graphs to allow a better visualization of the results

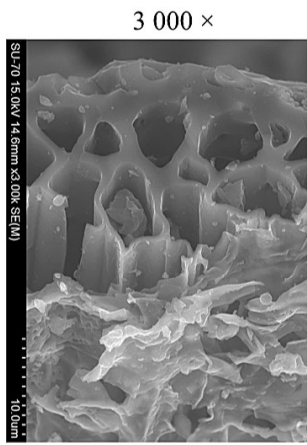
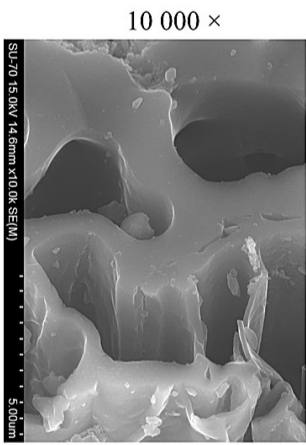
Fig. 3. Fittings for the isotherms experimental data for KOH-BW-800-150 in a) ultrapure water and b) wastewater; and for KOH-PL-800-150 in c) ultrapure water and d) wastewater. The results were fitted to Langmuir (solid lines) and Freundlich (dashed lines) equilibrium models. Each point (\pm standard deviation) is the average of three replicates. Note that x and y -axis scales are not the same in all graphs to allow a better visualization of the results



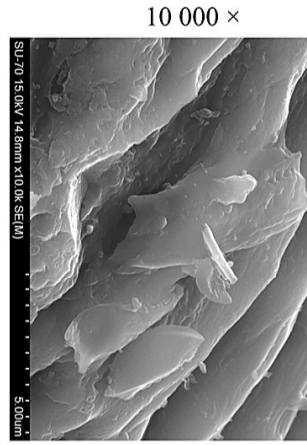
PL



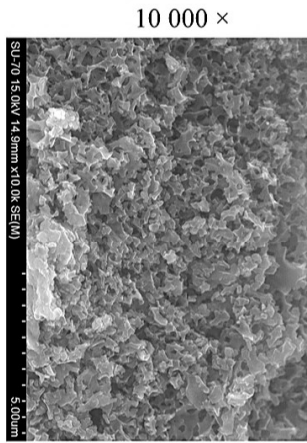
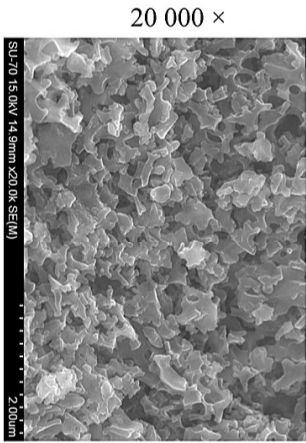
BW



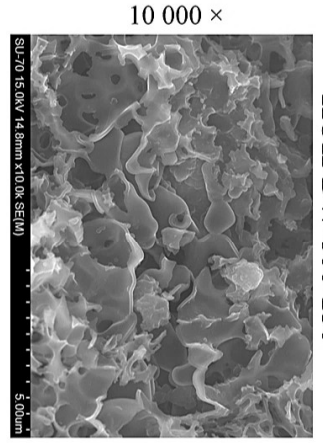
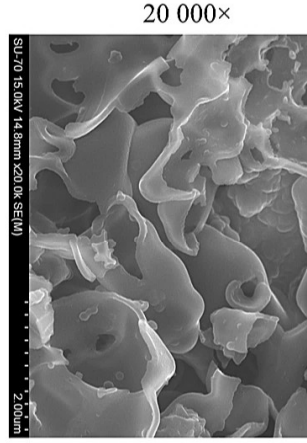
BC-PL-800-150



BC-BW-800-150

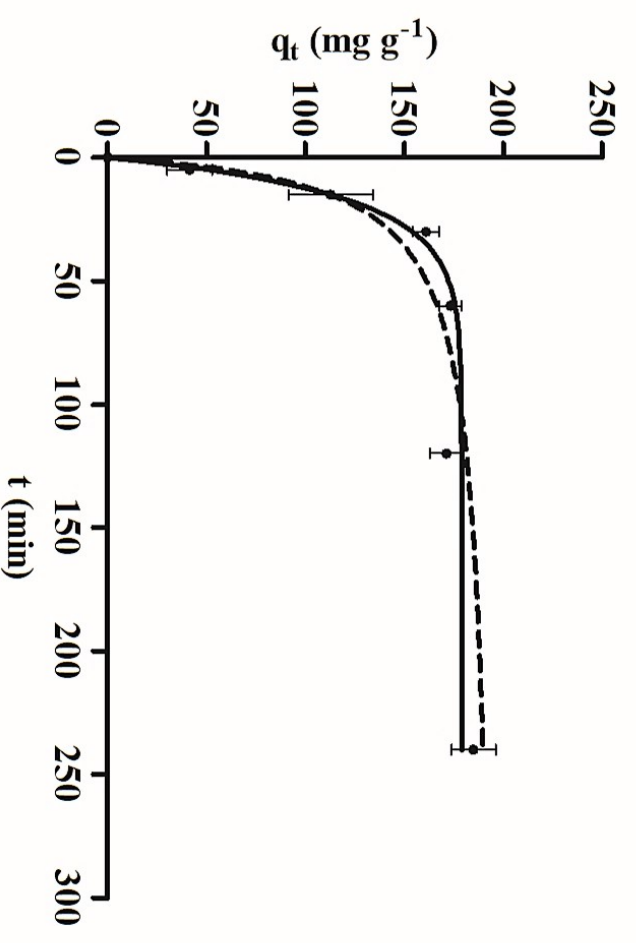


KOH-PL-800-150

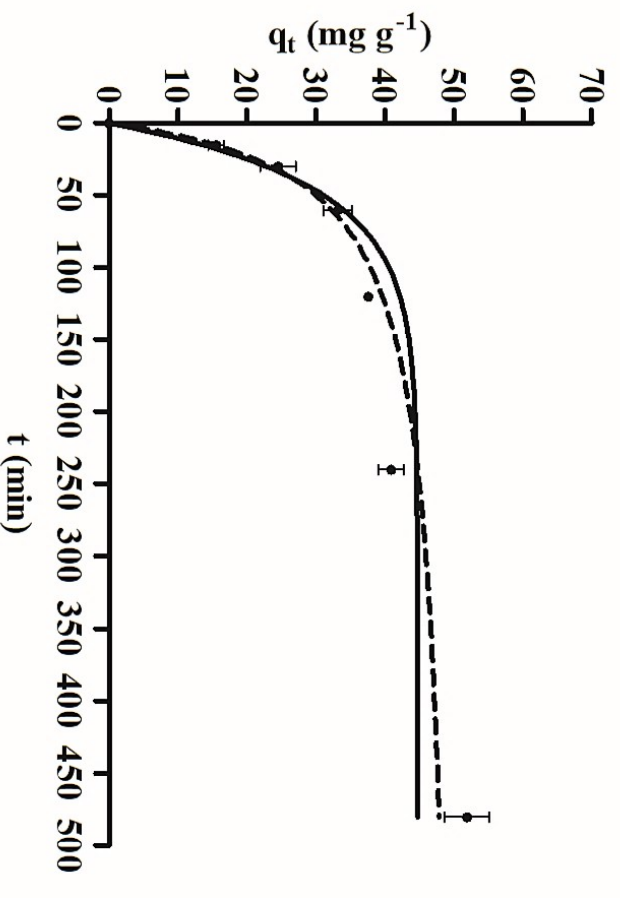


KOH-BW-800-150

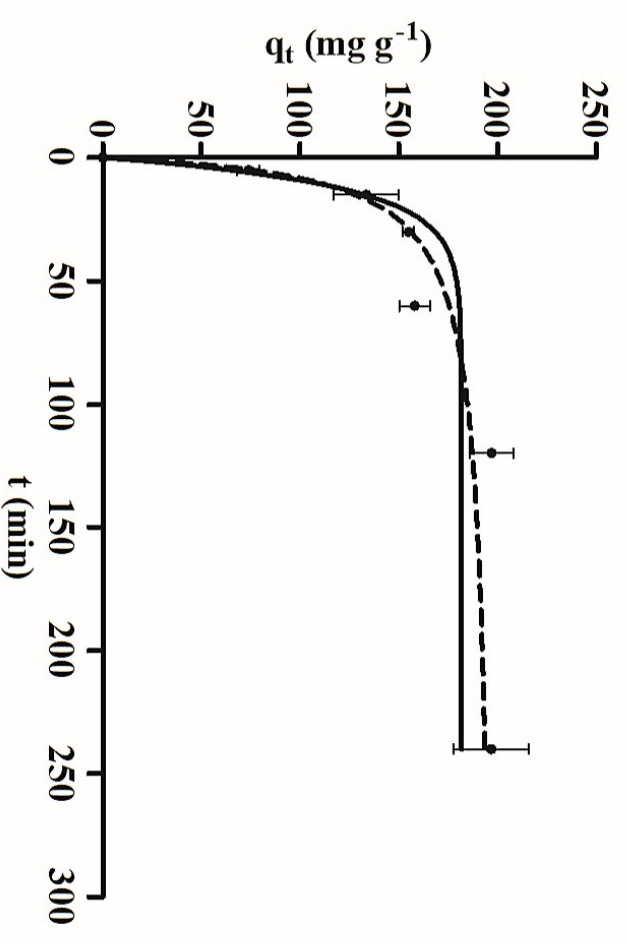
a)



b)



c)



d)

